



## OPEN ACCESS

EDITED BY  
Emilio Carbone,  
University of Turin, Italy

REVIEWED BY  
Michelino Puopolo,  
Stony Brook University, United States  
Bruce P. Bean,  
Harvard Medical School, United States

\*CORRESPONDENCE  
R. Ryley Parrish  
ryley\_parrish@byu.edu

SPECIALTY SECTION  
This article was submitted to  
Cellular Neurophysiology,  
a section of the journal  
Frontiers in Cellular Neuroscience

RECEIVED 09 June 2022  
ACCEPTED 31 August 2022  
PUBLISHED 29 September 2022

CITATION  
Thouta S, Waldbrook MG, Lin S,  
Mahadevan A, Mezeyova J, Soriano M,  
Versi P, Goodchild SJ and Parrish RR  
(2022) Pharmacological determination  
of the fractional block of Nav channels  
required to impair neuronal excitability  
and *ex vivo* seizures.  
*Front. Cell. Neurosci.* 16:964691.  
doi: 10.3389/fncel.2022.964691

COPYRIGHT  
© 2022 Thouta, Waldbrook, Lin,  
Mahadevan, Mezeyova, Soriano, Versi,  
Goodchild and Parrish. This is an  
open-access article distributed under  
the terms of the [Creative Commons  
Attribution License \(CC BY\)](https://creativecommons.org/licenses/by/4.0/). The use,  
distribution or reproduction in other  
forums is permitted, provided the  
original author(s) and the copyright  
owner(s) are credited and that the  
original publication in this journal is  
cited, in accordance with accepted  
academic practice. No use, distribution  
or reproduction is permitted which  
does not comply with these terms.

# Pharmacological determination of the fractional block of Nav channels required to impair neuronal excitability and *ex vivo* seizures

Samrat Thouta<sup>1</sup>, Matthew G. Waldbrook<sup>1</sup>, Sophia Lin<sup>1</sup>,  
Arjun Mahadevan<sup>1</sup>, Janette Mezeyova<sup>1</sup>, Maegan Soriano<sup>1</sup>,  
Pareesa Versi<sup>1</sup>, Samuel J. Goodchild<sup>1</sup> and R. Ryley Parrish<sup>1,2\*</sup>

<sup>1</sup>Department of Cellular and Molecular Biology, Xenon Pharmaceuticals Inc., Burnaby, BC, Canada,  
<sup>2</sup>Department of Cell Biology and Physiology, Brigham Young University, Provo, UT, United States

Voltage-gated sodium channels (Nav) are essential for the initiation and propagation of action potentials in neurons. Of the nine human channel subtypes, Nav1.1, Nav1.2 and Nav1.6 are prominently expressed in the adult central nervous system (CNS). All three of these sodium channel subtypes are sensitive to block by the neurotoxin tetrodotoxin (TTX), with TTX being almost equipotent on all three subtypes. In the present study we have used TTX to determine the fractional block of Nav channels required to impair action potential firing in pyramidal neurons and reduce network seizure-like activity. Using automated patch-clamp electrophysiology, we first determined the IC<sub>50</sub>s of TTX on mouse Nav1.1, Nav1.2 and Nav1.6 channels expressed in HEK cells, demonstrating this to be consistent with previously published data on human orthologs. We then compared this data to the potency of block of Nav current measured in pyramidal neurons from neocortical brain slices. Interestingly, we found that it requires nearly 10-fold greater concentration of TTX over the IC<sub>50</sub> to induce significant block of action potentials using a current-step protocol. In contrast, concentrations near the IC<sub>50</sub> resulted in a significant reduction in AP firing and increase in rheobase using a ramp protocol. Surprisingly, a 20% reduction in action potential generation observed with 3 nM TTX resulted in significant block of seizure-like activity in the 0 Mg<sup>2+</sup> model of epilepsy. Additionally, we found that approximately 50% block in pyramidal cell intrinsic excitability is sufficient to completely block all seizure-like events. Furthermore, we also show that the anticonvulsant drug phenytoin blocked seizure-like events in a manner similar to TTX. These data serve as a critical starting point in understanding how fractional block of Nav channels affect intrinsic neuronal excitability and seizure-like activity. It further

suggests that seizures can be controlled without significantly compromising intrinsic neuronal activity and determines the required fold over  $IC_{50}$  for novel and clinically relevant Nav channel blockers to produce efficacy and limit side effects.

#### KEYWORDS

sodium channel, tetrodotoxin, epileptiform activity, multiarray electrophysiology, inhibition, pharmacology

## Introduction

Voltage-gated ion channels form the basis for electrical activity in cells (Catterall, 1995; Armstrong and Hille, 1998). Specifically, voltage-gated sodium (Nav) channels are critical for action potential generation in excitable tissues (de Lera Ruiz and Kraus, 2015; Kwong and Carr, 2015). There are three predominant Nav channel genes expressed in the adult brain, denoted *SCN1A*, *SCN2A* and *SCN8A*, which encode the channels Nav1.1, Nav1.2 and Nav1.6, respectively (Goldin et al., 2000; Trimmer and Rhodes, 2004; Wang et al., 2017). These channels are expressed differentially in the central nervous system: Nav1.2 and Nav1.6 are expressed in excitatory neurons (Caldwell et al., 2000; Hu et al., 2009; Tian et al., 2014; Katz et al., 2018) while Nav1.1 is the major channel in inhibitory interneurons (Yu et al., 2006; Ogiwara et al., 2007; Catterall et al., 2010). These channels are critical for normal physiological function of neuronal network activity and alterations in their function can result in aberrant network activity. For example, gain of function mutations of both the Nav1.2 (Kearney et al., 2001; Misra et al., 2008; Ogiwara et al., 2009; Liao et al., 2010) and Nav1.6 (O'Brien and Meisler, 2013; Gardella and Moller, 2019; Johannesen et al., 2019) have been demonstrated to cause severe epilepsies, while loss of function mutations of Nav1.1 is the main cause of Dravet syndrome (Catterall et al., 2010; Bender et al., 2012; Cheah et al., 2012; Catterall, 2018). Additionally, loss of function of Nav1.2 or Nav1.6 can result in neuronal disorders such as autism spectrum disorder, demonstrating that balance between excitation and inhibition must be maintained within the brain (Larsen et al., 2015; Ben-Shalom et al., 2017).

Despite the risk of causing cardiac, behavioral, or cognitive side effects, a large number of Nav channel blockers are used as antiepileptic drugs (AEDs) (Zuliani et al., 2009; Khateb et al., 2021). All the currently available AEDs on the market that inhibit Nav channels are not selective between the Nav isoforms (pan-Nav). Our group has recently demonstrated the utility in animal models of a subtype specific Nav1.6 channel inhibitor which is

effective at limiting seizures with a wider therapeutic margin compared with conventional pan-Nav AEDs (Johnson et al., 2022). However, these isoform selective Nav inhibitors are not yet available in the clinic. To further our understanding of Nav targeting AEDs, we sought to determine the minimal fractional block of Nav current required to limit seizure activity and how that impacts single cell intrinsic excitability. Here, we investigated this using the tool compound tetrodotoxin (TTX), which is approximately equipotent on all three predominantly expressed Nav channels in the adult brain and shows only mild state dependent block without significant changes in the affinity between resting and inactivated states (Huang et al., 2012). As this study would be conducted using mouse brain slices, we first characterized the potency of TTX on mouse Nav1.1, Nav1.2, and Nav1.6 channels expressed in HEK 293 cells using automated-patch clamp electrophysiology. We found the potency to be similar across Nav1.1, 1.2 and 1.6, consistent with the reported values on human sodium channels. Next, using brain slice electrophysiology, we also determined the efficacy of TTX in suppressing intrinsic neuronal excitability and showed that it required nearly 80% block of  $Na^+$  current to significantly reduce action potential firing in pyramidal cells and 100% block of  $Na^+$  current to fully block firing upon depolarizing current injections. However, using a ramp protocol, we found that approximately a 20% reduction in available sodium current can reduce action potential firing and right shift the rheobase. We next sought to determine the fractional block of Nav channels required to limit *ex vivo* seizure activity. Interestingly, we found that the zero  $Mg^{2+}$  model of epilepsy is more sensitive to sodium channel block than cell intrinsic properties, where a 20% reduction of Nav currents significantly reduced *ex vivo* seizure generation. These data demonstrate a discrepancy between somatic action potential firing and initiation of seizure-like activity. It also indicates that seizure control might be achieved without significantly compromising cell intrinsic properties and demonstrates a non-linearity in the relationship between Nav channel availability, neuronal excitability, and seizure-like activity suppression.

## Materials and methods

### Electrophysiology using HEK 293 cells

The potency of TTX on mouse Nav channel subtypes was assessed using a Qube 384 (Sophion) automated voltage-clamp platform. HEK-293 cell lines stably expressing Nav1.x channels correspond to the following GenBank accession numbers: mouse Nav1.1 (NM\_018733.2), mouse Nav1.2 (NP\_001092768.1) and mouse Nav1.6 (NM\_001077499). The Nav  $\beta$ 1 subunit (NM\_199037) was co-expressed in all cell lines. Mouse Nav1.6 channels were also co-expressed with FHF2B (NM\_033642) to increase functional expression. To measure the TTX-inhibition of Nav channels, the membrane potential was maintained at a voltage ( $-120$  mV) where channels are mainly at rest followed by a depolarization for 10 s to the empirically determined  $V_{0.5}$  for that cell followed by a test pulse to  $-20$  mV for 5 ms to activate the Nav channels and quantify the TTX inhibition of the current. The protocol was repeated every 30 s. The  $V_{0.5}$  of steady state inactivation was determined using the Qube adaptive  $V_{0.5}$  function with a series of 500 ms depolarizing steps from a holding potential of  $-120$  mV to  $-20$  mV in 10 ms steps with a test pulse to  $-20$  mV to evaluate voltage dependence of availability. The availability curve was fit with a Boltzmann charge-voltage equation to find the  $V_{0.5}$ . To construct the TTX concentration response curves, baseline currents were established in vehicle for 5 min (0.5% DMSO) before addition of the appropriate TTX concentration for 5 min. Full inhibition response amplitudes were determined by adding tetrodotoxin (TTX, 300 nM) to each well at the end of the experiment. The fractional inhibition by TTX was calculated by normalizing the response in different concentrations of TTX to the baseline vehicle current and the full inhibition response in a supramaximal concentration of 300 nM TTX. Appropriate filters for minimum seal resistance were applied (typically  $> 500$  M $\Omega$  membrane resistance), and series resistance was compensated at 100%. Experiments were performed at 30°C. Currents were sampled at 25 kHz and low pass filtered at 5 kHz.

### Automated patch-clamp recording solutions

The recording solutions for Nav1.1, Nav1.2, and Nav1.6 cell line studies contained: Intracellular solution (ICS): 5 mM NaCl, 10 mM CsCl, 120 mM CsF, 0.1 mM CaCl<sub>2</sub>, 2 mM MgCl<sub>2</sub>, 10 mM HEPES [4-(2-hydroxyethyl)-1-piperazineethanesulfonic acid buffer], 10 mM EGTA (ethylene glycol tetra acetic acid); adjusted to pH 7.2 with CsOH. Extracellular solution (ECS): 140 mM NaCl, 5 mM KCl, 2 mM CaCl<sub>2</sub>, 1 mM MgCl<sub>2</sub>, 10 mM HEPES; adjusted

to pH 7.4 with NaOH. Osmolarity for the ICS and ECS solutions was adjusted with glucose to 300 mOsm/kg and 310 mOsm/kg, respectively.

### Animals

All animal handling and experimentation involving animals were conducted using approved protocols according to the guidelines of the Canadian Council on Animal Care (CCAC) and approved by the Xenon Animal Care Committee (XACC). Brain slice electrophysiology and MEA experiments were performed on male or female CF-1<sup>TM</sup> mice (3–5 weeks old, Charles River). All the mice colonies were maintained in the Animal Resource Facility at Xenon Pharmaceuticals. Mice were given food and water *ad libitum* and kept on a 12-h light/dark cycle.

### Acute brain slice preparation

Mice were deeply anesthetized with isoflurane [5% (vol/vol) in oxygen] and decapitated. The brain was removed and transferred immediately into an ice cold oxygenated (95% O<sub>2</sub>, 5% CO<sub>2</sub>) sucrose cutting solution containing the following (in mM): 214 Sucrose, 26 NaHCO<sub>3</sub>, 1.6 NaH<sub>2</sub>PO<sub>4</sub>, 11 Glucose, 2.5 KCl, 0.5 CaCl<sub>2</sub>, 6 MgCl<sub>2</sub>, adjusted to pH 7.4. 300  $\mu$ m-thick neocortical coronal/horizontal slices were collected for the patch-clamp studies and 350  $\mu$ m-thick neocortical horizontal slices were collected for the MEA studies, cut using a VT1200 vibratome (Leica). The slices were then incubated in artificial cerebral spinal fluid (aCSF) containing (in mM): 126 NaCl, 3.5 KCl, 26 NaHCO<sub>3</sub>, 1.26 NaH<sub>2</sub>PO<sub>4</sub>, 10 Glucose, 1 MgCl<sub>2</sub>, 2 CaCl<sub>2</sub>, pH 7.4 with 95% O<sub>2</sub>-5% CO<sub>2</sub> at 34°C for 45 min prior to recording.

### Brain slice patch-clamp electrophysiology

After incubation in aCSF for  $\sim 45$  min, individual slices were transferred to the recording chamber and constantly perfused at 2 ml/min with oxygenated aCSF maintained at 34°C. The neurons were visualized with infrared differential interference contrast (IR-DIC; Slicescope Pro 2000, Scientifica, United Kingdom) in combination with a 40X water immersion objective. Cortical pyramidal neurons were identified based on their characteristic large, triangular soma and single apical dendrite. Whole-cell patch clamp recordings were performed using a Multiclamp 700 B amplifier and signals were digitized and acquired using Digidata 1550B and pClamp 11 software (Molecular Devices). The recording chamber was grounded with an

Ag/AgCl pellet. Patch pipettes (4–6 M $\Omega$ ) were pulled from borosilicate glass using a P-70 micropipette puller (Sutter Instruments).

Intrinsic neuronal excitability was recorded in current-clamp mode using an internal recording solution containing the following (in mM): 120 K<sup>+</sup> Gluconate, 10 HEPES, 1 MgCl<sub>2</sub>, 1 CaCl<sub>2</sub>, 11 KCl, 11 EGTA, 4 MgATP, 0.5 Na<sub>2</sub>GTP, pH adjusted to 7.2 using KOH and osmolarity adjusted to 290 mOsm/kg using D-mannitol. To record the intrinsic excitability of pyramidal neurons, the following synaptic blockers were added; NMDA receptor antagonist D-2-amino-5-phosphonovalerate (D-APV, 50  $\mu$ M), AMPA receptor antagonist 6,7-dinitroquinoxaline-2,3-dione (NBQX, 10  $\mu$ M) and GABA<sub>A</sub> receptor antagonist gabazine (10  $\mu$ M) were added to the aCSF. The liquid junction potential was + 13.3 mV (bath potential relative to pipette), and the data was reported without subtraction. Bridge balance values were monitored during recordings and cells displaying bridge balance values > 20 M $\Omega$  were excluded from the analysis. Changes in intrinsic excitability were evaluated by using a current step and a ramp protocol. In case of step protocol, action potentials were evoked with 1 s long square-pulse current injections from –100 to 440 pA in 20 pA increments. A current ramp protocol of varying slopes (60, 120 and 240 pA/s—0 to 480 pA) was also used to evoke AP firing. Data under current clamp conditions were sampled at 50 kHz and low pass filtered at 10 kHz. Once baseline AP firing was determined in the extracellular recording solution (aCSF), the TTX with different concentrations was washed onto the slice for 15 min and the AP-generating protocol was repeated.

For recording Na<sup>+</sup> currents in pyramidal neurons in voltage-clamp mode, the external Na<sup>+</sup> concentration was reduced from physiological level to 50 mM. This low Na<sup>+</sup> concentration improves the voltage-clamp in pyramidal neurons, which produce large Na<sup>+</sup> currents. However, it is still not possible to achieve optimal voltage clamp in an intact neuron. The modified aCSF contained the following (in mM): 50 NaCl, 90 TEA-Cl, 10 HEPES, 2 CaCl<sub>2</sub>, 2 MgCl<sub>2</sub>, 3.5 KCl, 3 CsCl, 0.2 CdCl<sub>2</sub>, 4 4-aminopyridine, 25 Glucose, pH adjusted to 7.2 using NaOH. The internal solution contained the following (in mM): 110 CsF, 10 HEPES, 11 EGTA, 2 MgCl<sub>2</sub>, 0.5 NaGTP, 2 Na<sub>2</sub>ATP, pH adjusted to 7.2 with CsOH. Data under voltage clamp conditions were sampled at 20 kHz and low pass filtered at 2 kHz. Leakage and capacitive currents were automatically subtracted using a pre-pulse protocol (-P/4).

## Multi-electrode array recordings

Recordings were performed on the 3Brain BioCAM DupleX system (Switzerland) using the 3Brain Accura HD-MEA chips with 4,096 electrodes at a pitch of 60  $\mu$ m. Slices were placed

onto the electrodes with a harp placed on top to keep the slice pressed down gently to the recording electrodes. Slices were perfused continuously with a zero Mg<sup>2+</sup> artificial cerebrospinal fluid (aCSF) to induce epileptiform activity. TTX and phenytoin was bath applied 10 min prior to washout of Mg<sup>2+</sup> ions. Recordings were obtained from the entire neocortical slice. Recordings were performed at 33–36°C. The solutions were perfused at the rate of 5.0 mL/min. Signals were sampled at 10 kHz with a high-pass filter at 2 Hz. All analysis was done in our custom-made GUI (Mahadevan et al., 2022).

## Data analysis and statistics

Brain slice patch clamp electrophysiology recordings were analyzed using Clampfit 11 (Molecular devices) and a custom-made GUI written in Python version 3.7. Python script can be made available upon request. The number of APs was measured and plotted as a function of current stimulus to allow comparison between vehicle and TTX treatment. Rheobase was measured as the minimum intensity of 1 s current pulse required for initiation of AP. The AP threshold voltage was defined as the voltage at which the first derivative of the AP waveform (dv/dt) reached 10 mV/ms. The threshold was calculated at rheobase current. For AP waveform analysis, amplitude was measured from threshold to peak, and AP width measurements were made at 50% of the peak amplitude. AP upstroke velocity was assessed through phase plots that were generated using the membrane potential trace and the dV/dt trace.

All statistical analyses were performed using GraphPad Prism 7 software and differences with *p*-value < 0.05 were considered statistically significant. All the figures were created using diagrams, Inkscape 1.1. and all the data are expressed as mean  $\pm$  SEM. The *n* value represents the number of cells tested for the patch clamp data or number of slices for the MEA data. For the statistical comparisons of the *i*-o curves, the differences observed between the vehicle versus TTX treated conditions was evaluated by two-way ANOVA with a Dunnett's multiple comparisons test. The statistical analysis of the effect of TTX on the AP properties was evaluated using a One-way ANOVA (Figures 3D–G) and paired two-tail *t*-test (Figures 4B–E). MEA data was analyzed using a One-way ANOVA with a Dunnett's test.

## Pharmacological agents

D-AP5, NBQX and Gabazine were purchased from Hellobio. Tetrodotoxin (TTX) was purchased from Biotrend. Phenytoin was purchased from Sigma-Aldrich. All drugs were prepared as stock solutions and stored at –20°C; aliquots were

thawed and added to aCSF to the working concentrations. Drugs were applied by bath perfusion at a flow rate of 2 ml/min.

## Results

### TTX inhibition of mouse Nav channels expressed in central nervous system

Previous studies reported the potency of TTX on rat or human Nav channel isoforms (Rosker et al., 2007; Zhang et al., 2013; Tsukamoto et al., 2017), however, the potency on the mouse neuronal Nav channel isoforms, to our knowledge, has not been reported in the same publication under the same experimental conditions. Here, using automated patch-clamp electrophysiology, we assessed the potency of TTX on the mouse Nav isoforms that are highly expressed in the CNS including: Nav1.1, 1.2, and 1.6 (Ogiwara et al., 2007; Hu et al., 2009; Dutton et al., 2013; Tian et al., 2014).

To assess the potency, we first measured the concentration responses of TTX using a voltage-clamp protocol that holds channels at the  $V_{0.5}$  of inactivation, where the population of channels are approximately equally distributed between resting and inactivated states as described in the “Materials and methods” section. The  $V_{0.5}$  for each channel was as follows: mNav1.1  $-54.4 \pm 0.6$  mV ( $n = 79$ ), mNav1.2  $-61.3 \pm 0.9$  mV ( $n = 45$ ) and mNav1.6  $-61.9 \pm 0.8$  mV ( $n = 42$ ). This is to better simulate membrane potentials that are found in neurons that will typically have resting membrane potentials where channels are in mixed states. Representative current traces at approximately  $IC_{50}$  concentrations for each subtype tested are shown in **Figure 1A** (red trace). Complete block of  $Na^+$  current was observed by application of 300 nM TTX (green trace). The concentration-response relationship for the mNav1.1, 1.2 and 1.6 channels are plotted in **Figure 1B**. To construct the concentration-response, individual cells were exposed to single concentrations of TTX, normalizing the inhibition of each cell to its own vehicle baseline at each concentration. This data was then pooled, and the mean data was fit with a Hill-Langmuir equation. TTX potently inhibited mNav1.6 channels with an  $IC_{50}$  of 0.6 nM (95% CI: 0.5 to 0.7 nM). Inhibition of other mNav1.X isoforms required somewhat higher concentrations of TTX with  $IC_{50}$ s of 2.6 nM (95% CI: 1.9 to 3.5 nM) for mNav1.1, and 4.9 nM (95% CI: 3.8 to 6.5 nM) for mNav1.2. The potency in mouse Nav channels was similar to those seen in human orthologs with low nanomolar  $IC_{50}$  of TTX on hNav1.6 and 1.1, and slightly higher potency on hNav1.2. The observed  $IC_{50}$ s for TTX inhibition were 1.43 nM (95% CI: 0.8 to 2.3 nM) for hNav1.1, 2.5 nM (95% CI: 1.6 to 4 nM) for hNav1.2 and 0.5 nM (95% CI: 0.4 to 0.6 nM) for hNav1.6. These data on human Nav isoforms are consistent with those reported previously (Tsukamoto et al., 2017). We also tested the TTX potency at a membrane potential of  $-120$  mV, where the channels are

fully in the resting state. The data revealed that potency was reduced by 2.5-fold from 2.6 nM to 6.6 nM for mNav1.1, 6.2-fold from 4.9 nM to 30.7 for mNav1.2 and 1.5-fold from 0.6 nM to 0.9 nM for mNav1.1 respectively. These data support the mild voltage dependency of TTX on Nav channels previously reported (Huang et al., 2012).

### Inhibition of TTX on $Na^+$ currents and AP firing in pyramidal neurons in brain slices

After the characterization of TTX potency in heterologously expressed mouse Nav channels, we moved to electrophysiological analysis of neuronal Nav currents in the physiologically appropriate environment of acute brain slices. We made whole-cell patch clamp recordings of excitatory pyramidal neurons from coronal slices, in which Nav1.2 and Nav1.6 channels are predominantly expressed (Hu et al., 2009; Tian et al., 2014; Katz et al., 2018; Spratt et al., 2021). Different concentrations of TTX (3, 10 and 30 nM) were tested to measure the sensitivity of  $Na^+$  currents to TTX. Representative whole-cell  $Na^+$  currents recorded from pyramidal neurons in response to a typical voltage-clamp step protocol is shown in **Figure 2A**. Application of increasing concentrations of TTX resulted in concentration-dependent inhibition in the  $Na^+$  peak current.  $Na^+$  currents were reduced to  $82.3 \pm 4.3\%$  of vehicle in 3 nM TTX ( $n = 8$ ),  $55.3 \pm 5.2\%$  of vehicle ( $n = 8$ ) in 10 nM TTX;  $21.6 \pm 3.3\%$  of vehicle ( $n = 7$ ) in 30 nM TTX and  $9.7 \pm 1.8\%$  of vehicle ( $n = 3$ ) in 100 nM TTX (**Figures 2A,B**). The concentration-response curve for TTX on  $Na^+$  currents from pyramidal neurons was constructed and fitted with a Hill-Langmuir equation giving an  $IC_{50}$  value of 9.2 nM (95% CI: 7.6 to 11 nM) (**Figure 2B**). This result is comparable to the potency of TTX on heterologously expressed channels (**Figure 1**) and other reported effects of TTX on  $Na^+$  currents in isolated CA1 pyramidal neurons ( $IC_{50} = 6.4$  nM) (Madeja, 2000) and GABAergic neurons ( $IC_{50} = 7.2$  nM) of the substantia nigra obtained in nucleated patches (Seutin and Engel, 2010).

To determine the potency of TTX on AP firing, we next performed current-clamp recordings from the soma of pyramidal neurons in the presence of the synaptic blockers NBQX (10  $\mu$ M), AP5 (50  $\mu$ M) and Gabazine (10  $\mu$ M). **Figure 3A** shows the representative voltage responses to 220 pA current injection step in vehicle conditions and in the presence of different concentrations of TTX (3, 10 and 30 nM). Application of 10 nM TTX significantly reduced the number of APs by almost 60% across a range of stimuli and in 30 nM TTX, depolarizing current did not elicit APs (**Figure 3B**). Interestingly, the lowest concentration of TTX (3 nM) blocked  $\sim 20\%$  of the  $Na^+$  current (**Figure 2**) but showed little or no effect on the AP firing (**Figure 3B**). A concentration-response relation for TTX block on AP firing at maximal current stimulus

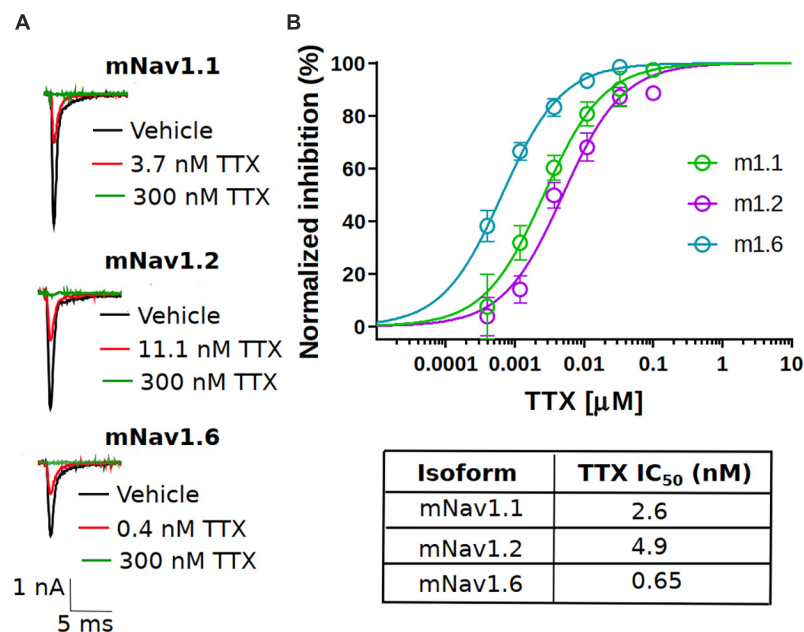


FIGURE 1

Potency of TTX inhibition on the mouse neuronal Nav channels. (A) Representative traces of voltage-clamp recordings of vehicle (black) and the concentration close to the TTX IC<sub>50</sub> (red) for mouse Nav channel isoforms (mNav1.1, mNav1.2 and mNav1.6) heterologously expressed in HEK293 cells. For all the tested Nav channel isoforms, 300 nM TTX (green trace) showed complete block of Na<sup>+</sup>-current.

(B) Concentration-response relationship for TTX inhibition of mouse Nav1.1, Nav1.2 and Nav1.6 channel isoforms. Each concentration represents the mean of  $n = 7-15$  cells. The solid line is the best fit of the average data to the Hill equation yielding IC<sub>50</sub> = 2.6 nM for mNav1.1, 4.9 nM for mNav1.2 and 0.65 nM for mNav1.6.

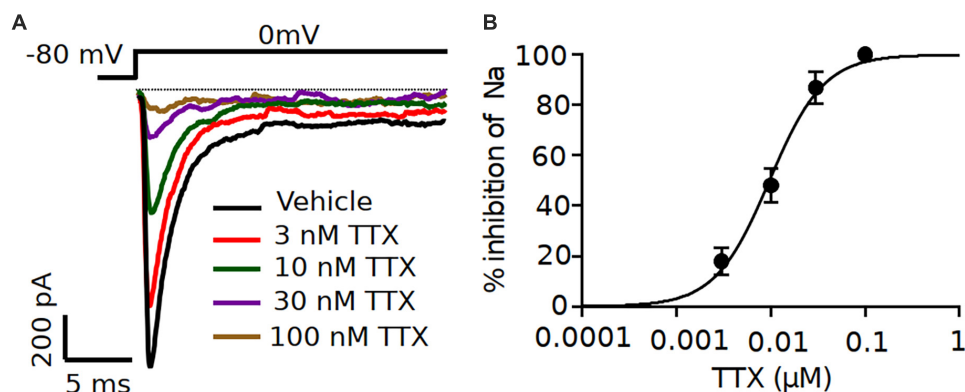


FIGURE 2

Increasing concentrations of TTX resulted in a concentration-dependent inhibition of Na<sup>+</sup> currents in mouse cortical pyramidal neurons.

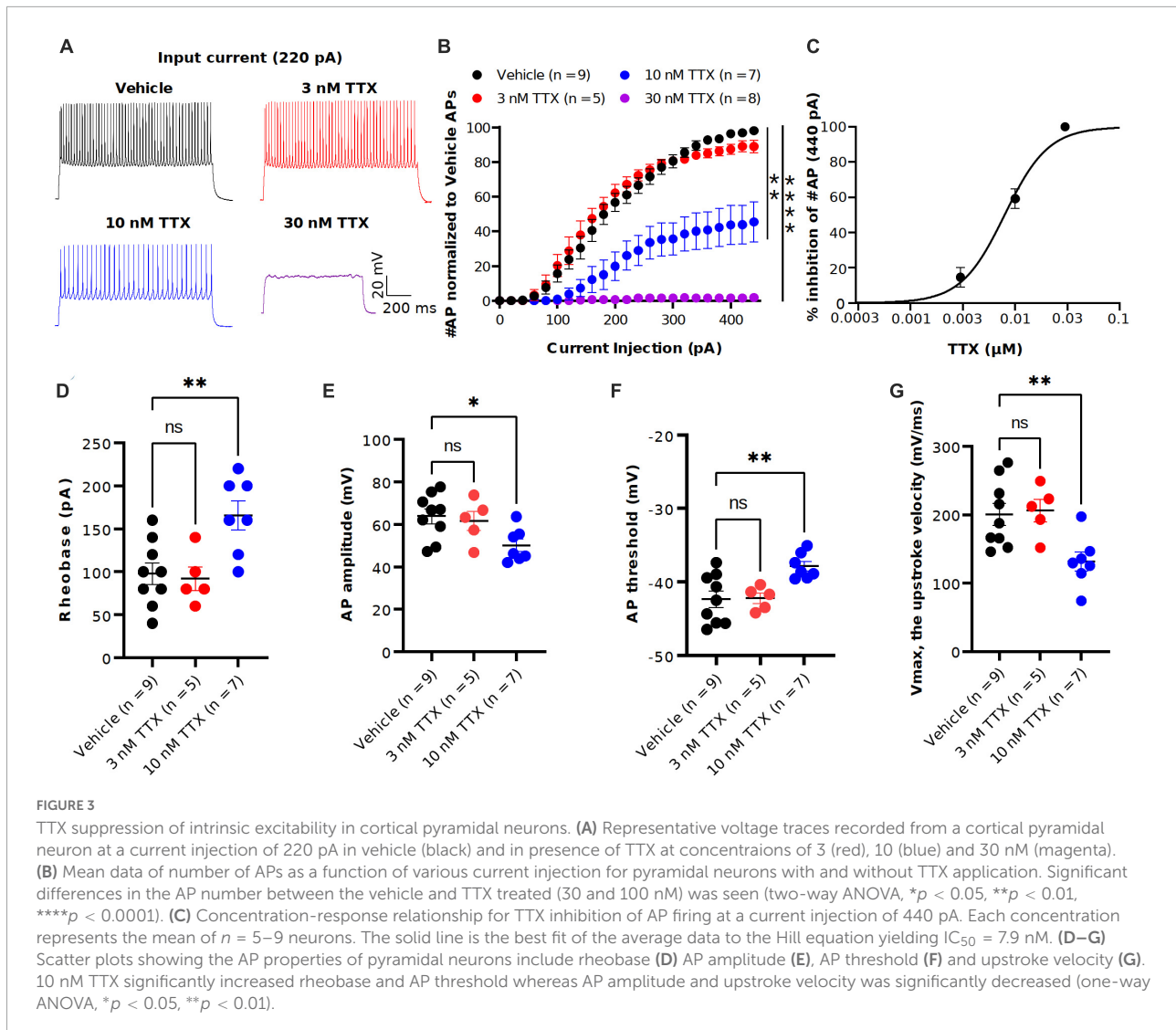
(A) Representative traces of Na<sup>+</sup> currents from pyramidal neurons recorded in vehicle condition and in presence of TTX at concentrations of 3, 10, 30 and 100 nM. Inhibition by TTX of Na<sup>+</sup> currents were elicited by a 20-ms pulse depolarized from a holding potential of -80 mV to 0 mV.

(B) Concentration-response relationship for TTX inhibition of Na<sup>+</sup> current in pyramidal neurons. Each point shows Na<sup>+</sup> peak current relative to vehicle averaged over 7 neurons, except for 100 nM TTX ( $n = 3$ ). The solid line is the best fit of the average data to the Hill equation yielding IC<sub>50</sub> = 9.2 nM.

(440 pA) revealed the half-maximal blocking concentration to be 7.9 nM (95% CI: 5.0 to 11 nM) (Figure 3C).

We next examined the passive and active parameters of AP firing. The resting membrane potential and input resistance were not altered by application of TTX (Table 1). Application

of 10 nM TTX increased significantly the rheobase (vehicle:  $112 \pm 25.7$  pA,  $n = 9$ ; 10 nM TTX:  $170 \pm 15.1$  pA,  $n = 7$ ,  $p < 0.05$ , Figure 3D) and AP threshold (vehicle:  $-41.4 \pm 1.3$  mV,  $n = 9$ ; 10 nM TTX:  $-36.1 \pm 1.7$  mV,  $n = 7$ ,  $p < 0.05$ , Figure 3F) whereas the AP amplitude (vehicle:  $63.0 \pm 3.2$  mV,  $n = 9$ ; 10



nM TTX:  $48.1 \pm 3.1$  mV,  $n = 7$ ,  $p < 0.05$ , **Figure 3E**) and maximum AP velocity (vehicle:  $200.6 \pm 16.2$  mV/ms,  $n = 9$ ; 10 nM TTX:  $132.4 \pm 12.1$  mV/ms,  $n = 7$ ,  $p < 0.05$ , **Figure 3G**) were significantly decreased. Together, these data suggest that it required nearly 80% block of  $Na^+$  current to significantly reduce AP firing and properties. Interestingly, low concentration of TTX showed very little effect of AP firing, whereas we did observe a significant block of  $Na^+$  current at 3 nM TTX (**Figure 2**).

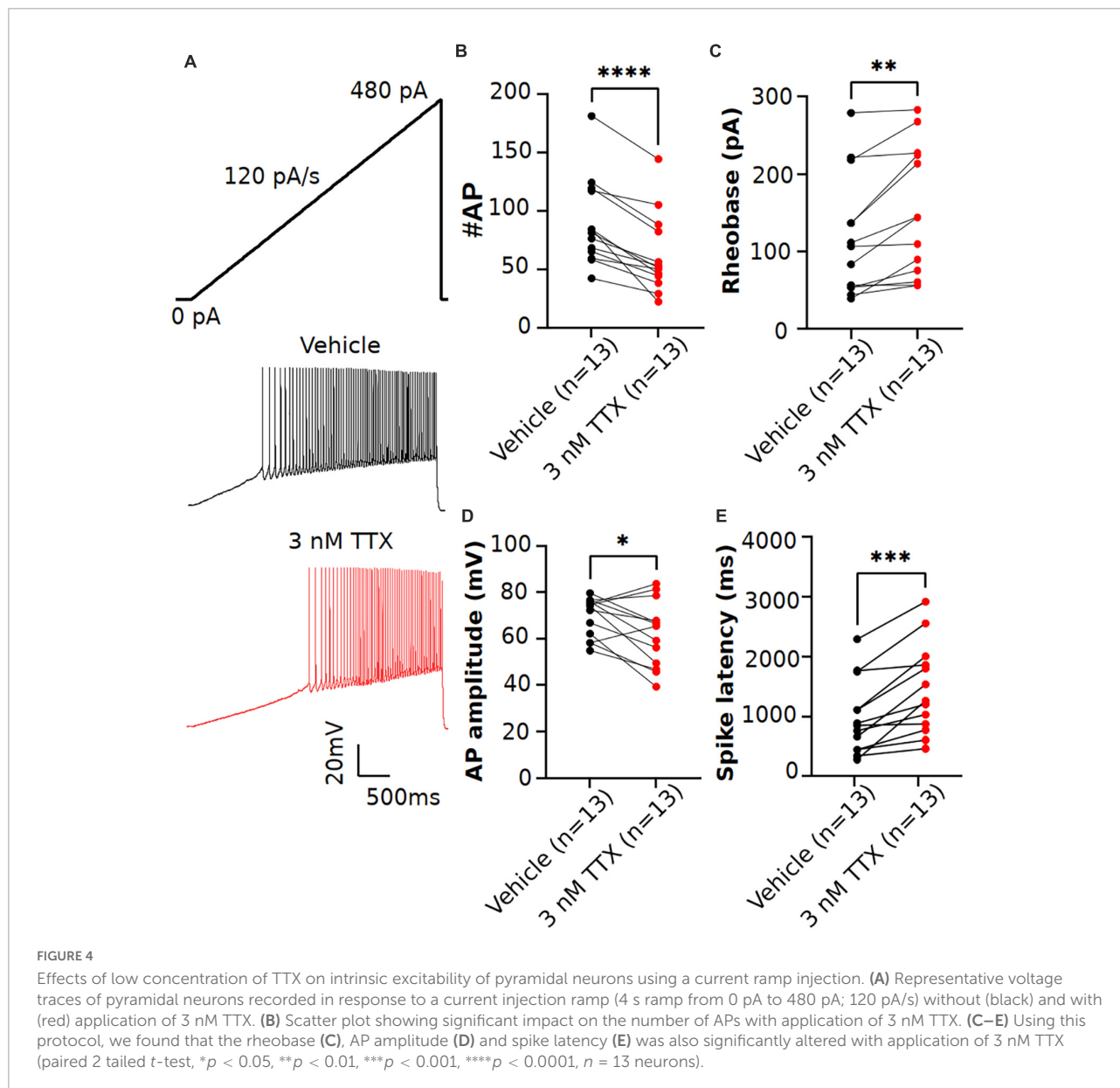
Previous studies in Purkinje neurons (Raman and Bean, 1999; Swensen and Bean, 2005) reported that low concentrations of TTX ( $\sim 3$  nM) significantly impacted AP firing. As shown in **Figure 3**, when measured using square-step current injection protocol, 3 nM TTX did not affect the number of APs or AP firing properties of pyramidal neurons. To further investigate the effects of TTX on neuronal excitability, we recorded AP firing using a slow ramp current injection. Application of 3 nM

TTX had no impact on resting membrane potential (vehicle:  $-68.2 \pm 1.03$  mV,  $n = 12$ ; 3 nM TTX:  $-68.3 \pm 1.3$  mV,  $n = 12$ ,  $p = 0.9$ , paired two-tail  $t$ -test). **Figure 4A** shows the representative voltage responses to a current ramp (4 s ramp from 0 to 480 pA; 120 pA/s) recorded from a pyramidal neuron in vehicle condition (black trace) and in the presence of 3 nM TTX (red trace). Unlike the step protocol (**Figure 3**), we found significant reduction in the number of APs with addition of 3 nM TTX compared to that of vehicle (**Figure 4B**) suggesting the ramp is a more sensitive assay of  $Na^+$  channel contributions to excitability. In addition, the rheobase and latency to first spike was increased significantly over vehicle whereas the AP amplitude was decreased (**Figures 4C-E**). This result suggests that 20% reduction of  $Na^+$  current is sufficient to influence neuronal excitability of pyramidal neurons when measured using a ramp protocol. Furthermore, to rule out any possible time-dependent changes in neuronal excitability

TABLE 1 Membrane characteristics of pyramidal neurons before (vehicle) and after application of various concentrations of TTX.

Parameter	Vehicle ( <i>n</i> = 9)	3 nM TTX ( <i>n</i> = 5)	10 nM TTX ( <i>n</i> = 7)	30 nM TTX ( <i>n</i> = 7)
RMP (mV)	-67.4 ± 0.7	-68.8 ± 1.3	-68.3 ± 1.6	-68.9 ± 1.6
R <sub>in</sub> (MΩ)	133.7 ± 17.6	139.6 ± 21.1	113.04 ± 10.4	139.3 ± 19.2

Data are presents as mean ± SEM. The number of cells tested with each condition is given in parenthesis. RMP, resting membrane potential; Rin, Input resistance.



we also recorded AP firing in response to a current ramp (0 to 480 pA; 120 pA/s) before and after 15 min application of vehicle solution. No changes in the neuronal excitability was observed during the period of vehicle application. The AP number was  $63.4 \pm 8.1$  (0 min) and  $75.2 \pm 8.3$  (15 min), *n* = 5, paired two-tail *t*-test, *p* = 0.46 (data not shown).

Because the rate of the current ramp could impact the Nav current availability (Park et al., 2013), we next recorded AP firing with current injection ramps of varying slopes (60, 120 and 240 pA/s) in the same cell, first in the vehicle condition, followed by the bath perfusion of 3 nM TTX. As shown in Table 2, regardless of ramp slope, we observed a significant reduction in the AP firing with 3 nM TTX. However, the percent inhibition of the AP

TABLE 2 Sensitivity of TTX on AP firing at different current ramp slopes.

Current ramp slopes	#AP		TTX inhibition of AP firing relative to vehicle (%)
	Vehicle ( <i>n</i> = 7)	3 nM TTX ( <i>n</i> = 7)	
60 pA/s	154 ± 19.5	126.8 ± 19.1*	18.0 ± 6.4
120 pA/s	82.8 ± 9.8	60.8 ± 9.05*	27.2 ± 4.1
240 pA/s	46.8 ± 5.1	32.1 ± 4.6*	32.3 ± 3.2

Data are presents as mean ± SEM. The number of cells tested is given in parenthesis. Asterisk (\*) indicate significant difference in the number of APs in 3 nM TTX condition from vehicle at a given ramp slope (two-tail *t*-test, \**p* < 0.05).

firing relative to vehicle is not significant different between the different current ramp rates. The percent inhibition of APs with 3 nM TTX relative to vehicle was 18.0%, 27.2% and 32.3% at current ramp slopes of 60, 120 and 240 pA/s, respectively (2-way ANOVA test with Dunnett's test).

## Inhibition of seizure-like events in TTX and phenytoin shows a clear concentration-dependent response

We next assessed the potency of TTX block of *ex vivo* seizure-like events, using a zero-magnesium aCSF solution. Removal of Mg<sup>2+</sup> ions typically results in seizure-like events in ~10–20 min. A representation of the seizure-like activity and the effects of various concentration of TTX is shown in Figure 5. Figure 5B displays representative raster plots from a slice in vehicle, and then 3 and 10 nM TTX respectively, demonstrating a decrease in epileptiform activity with increasing TTX concentration. The time-series traces over the entire 40-min recording period further demonstrate the loss of seizure-like events between vehicle and TTX bathed slices, suggesting 10 nM TTX is sufficient to block all seizure-like events (Figure 5C). Taking a closer look at the first seizure-like event from each treatment group, we also found that increasing TTX concentration appears to reduce higher frequency components during the seizure-like event, suggesting less neuronal recruitment during these pathological events (Figures 5D,E).

3 nM TTX is sufficient to significantly block seizure-like events, but 10 nM is required to completely prevent seizures from developing (Figure 6A). These data demonstrate that only a 20% reduction in Na<sup>+</sup> current in pyramidal cells can produce a significant reduction in seizure-like events, even when this results in a rather modest block of action potential firing in pyramidal cells (see Figures 3, 4). However, to fully achieve block of seizure-like events, it appears to require a 50% reduction in pyramidal cell Na<sup>+</sup> current. In addition to TTX, we also evaluated the potency of phenytoin (clinically approved anticonvulsant Na<sup>+</sup> channel blocker) required to block *ex vivo* seizure-like events, using concentrations of phenytoin that

match the same IC<sub>50</sub>s used for TTX (Kuo and Bean, 1994; Kuo et al., 1997). The data revealed that phenytoin blocked seizure-like events in a manner that is similar to TTX. 40 μM (threefold IC<sub>50</sub>) phenytoin significantly inhibited the seizure-like events, whereas 130 μM (10-fold IC<sub>50</sub>) completely blocked the seizure-like activity (Figure 6B). In summary, these findings demonstrate that only a partial block of pyramidal cell firing is required to achieve significant reductions in seizure-like events.

## Discussion

In the present study, we have demonstrated that relatively subtle reductions in pyramidal cell sodium current (~20%) are sufficient to significantly reduce *ex vivo* seizure-like activity. Interestingly, this 20% reduction in sodium current has relatively little effect on intrinsic excitability of pyramidal cells, where we found blocking ~80% of sodium current was required to impair neuronal firing with a standard step protocol. However, we also found that TTX sensitivity can be dependent on how the cell receives the current input, as a ramp protocol (Figure 4) demonstrated that neuronal action potentials can be significantly impaired at lower concentrations of TTX than a step protocol. This increased potency of TTX observed in our ramp protocol could be due to the mild voltage dependency of TTX that we and others have observed (Huang et al., 2012), suggesting that properties of the compound and how current is received by the cell will together dictate observed potency. Overall, our data suggests that subtle impairment of neuronal action potential firing with sodium channel blockers might be sufficient to reduce seizures, a finding that can be important for exploration of novel anticonvulsant compounds and when determining a therapeutically relevant dosing of compounds. To our knowledge, the current study is the first to determine the fractional block of Nav channels required to reduce neuronal excitability at both the cellular and network level. In addition, we have also assayed the potency of TTX at different levels of network and neuronal activity, providing novel insights into how pore Nav channel blockers behave during different forms of stimulation.

Of the available Nav inhibitors, we believe that TTX has good properties for tuning neuronal Nav currents due

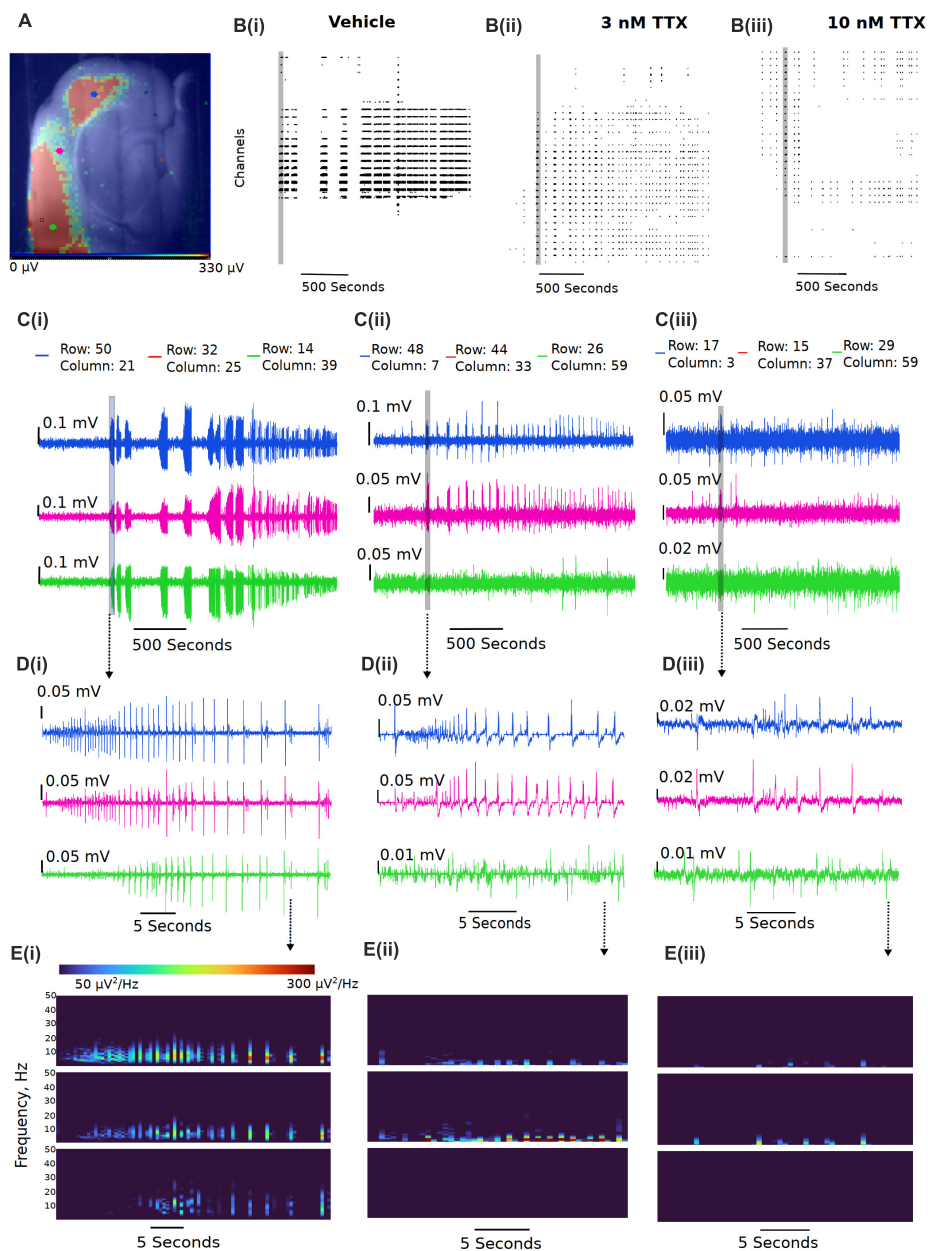


FIGURE 5

Representative reduction in seizure-like events following sodium current block by TTX. (A) Example slice from a multi-electrode array recording during a seizure-like event. Colored dots (blue, pink, and green dots) represent the approximate location of the selected traces. (B) Example raster plots from the entire recordings for the (Bi) 0  $\text{Mg}^{2+}$  vehicle, the (Bii) 3 nM TTX, and the (Biii) 10 nM TTX. (C) Example traces taken from either end of the neocortical slice (blue and green traces) and a trace selected from the middle of the slice (pink trace) for the (Ci) 0  $\text{Mg}^{2+}$  vehicle, the (Cii) 3 nM TTX, and the (Ciii) 10 nM TTX. (D) Zoomed in view of the first seizure-like events from each of the three treatment groups. (E) Spectral plots of the zoomed in seizure-like events in  $\mu\text{V}^2$ .

to the relatively low state dependence (Huang et al., 2012) compared with Nav targeting AEDs, which show much greater state dependence of at least 10X due to a higher affinity for inactivated state channels (Kuo and Bean, 1994; Kuo et al., 1997). TTX potency is therefore relatively stable across the ranges of membrane potentials that may be found between

different neurons and sub compartments. Several studies have demonstrated the potency of TTX on human and rat Nav1.6, 1.2, and 1.1 channels (Rosker et al., 2007; Tsukamoto et al., 2017; Zhang et al., 2013), however, this is the first report (to our knowledge) demonstrating the potency of TTX on these three mouse channel isoforms in an exogenously expressed system.

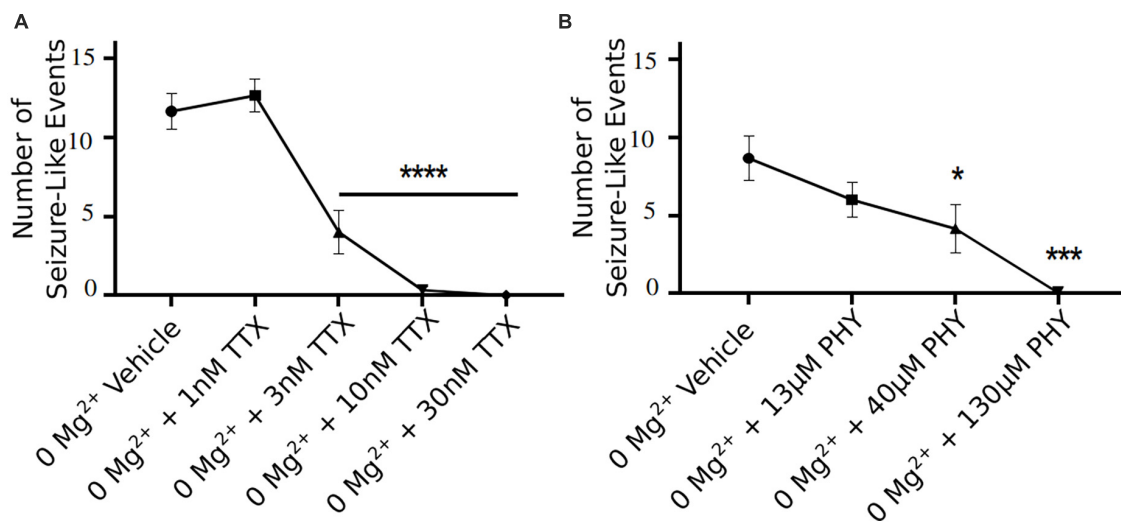


FIGURE 6

TTX and phenytoin (PHY) reduces seizure-like events in a clear concentration dependent manner. Seizure-like events are reduced in a TTX (A) and PHY (B) concentration-dependent manner (one-way ANOVA with a Dunnett's test, \* $p < 0.05$ , \*\*\* $p < 0.001$ , \*\*\*\* $p < 0.0001$ ,  $n = 6$  for TTX  $n = 5-7$  for PHY).

Our results on the mouse neuronal Nav channels are in line with what has been reported in both human and rat channels. These results allow for greater understanding and interpretation of data from mouse tissue when using TTX for partial block of Nav currents. It is also important to note that while we and others generally report TTX to be roughly equipotent on all three predominantly expressed Nav channels in the CNS, we did find an approximate 10X different in potency between inhibition of Nav1.6 vs Nav1.2 channels, consistent with the previous report on the inhibitory effects of TTX on human Nav 1.6 and Nav1.2 isoforms (Tsukamoto et al., 2017). Additionally, when assessing results from neuronal pan-sodium channel blockers, one must consider neuronal cell-type distribution of these channels. Nav1.6 and Nav1.2 channels are predominantly expressed in pyramidal cells (Caldwell et al., 2000; Hu et al., 2009; Tian et al., 2014; Katz et al., 2018) whilst Nav1.1 channels are the dominant sodium channel isoform in interneurons, particularly in the so-called fast spiking parvalbumin positive interneurons (Yu et al., 2006; Ogiwara et al., 2007). This data would suggest that pan-Nav channel blockers should reduce network excitability of all neuronal cell types, however, the network effect from this can be more complicated. Potent block of GABAergic neurons *via* suppression of Nav1.1 channels could result in pro-epileptic effects, as has been previously demonstrated (Patel et al., 2020). Nevertheless, pan-Nav channel blockers are effective anticonvulsant drugs in many situations, but their efficacy may be limited in situations with already impaired interneuron function. This is most clearly demonstrated by the fact that clinical approved sodium channel blockers are contraindicated in treatment of seizures associated with Dravet syndrome (Horn et al., 1986; Guerrini et al., 1998; Brunklaus

et al., 2012), a condition believed to be due to a reduction in Nav1.1 current. Interestingly, there is a body of literature that suggests in certain situations, interneurons can trigger seizure-like activity (Shiri et al., 2015; Yekhlief et al., 2015; Librizzi et al., 2017; Chang et al., 2018; Magloire et al., 2019). However, in the majority of physiological situations, it should be advantageous to preserve interneuron activity, where they provide on demand fast feed-forward inhibition to limit spreading seizures (Trevelyan et al., 2006; Cammarota et al., 2013; Sessolo et al., 2015; Parrish et al., 2018, 2019). Interestingly, there is evidence that TTX has milder effects on somatic AP firing of fast-spiking interneurons and that other pan-Nav blockers have a limited effect on the GABAergic network compared to the glutamatergic network (Pothmann et al., 2014; Kaneko et al., 2022). This could explain why we found that lower concentration of TTX is required to significantly limit seizure-like events compared to concentrations required to limit intrinsic excitability of pyramidal cells. Additionally, while our pyramidal cell intrinsic excitability study assays axonal initial segment (AIS) and somatic excitability, seizure like-events are network level events, where dendrites, axons, and postsynaptic release of neurotransmitters are also critical components of seizure propagation. For example, dendritic plateauing has been shown to be necessary for seizure generation, suggesting important network changes required for this type of pathological activity (Graham et al., 2021). Furthermore, axonal propagation of action potentials in neurons has been demonstrated to be more sensitive to sodium channel block than somatic action potentials (Hu and Jonas, 2014; Kaneko et al., 2022). Therefore, it is possible that lower concentrations of TTX impairs these other important network

components required for seizure genesis more profoundly than it does at the cell soma and the AIS, but this has not been studied in detail. Importantly, we also found that phenytoin, a clinically used anticonvulsant drug, blocked seizure-like events at similar concentrations relative to the IC<sub>50</sub> to TTX. This data further demonstrates that partial block of Nav channels is sufficient to reduce seizure-like events.

In conclusion, we have characterized the fractional block of sodium channels required to reduce the neuronal excitability of pyramidal cells and *ex vivo* seizure-like events using the tool compound TTX. This data could be helpful in assaying dose requirements to reduce seizures with clinically relevant Nav channel inhibitors. Currently, only pan-Nav channel blockers are available for clinical use, which, like TTX and phenytoin, are not highly selective. Whilst we await the assessment of isoform selective Nav inhibitors as effective AEDs, we need a better understanding of relevant exposures of pan-Nav blockers that may reduce seizures while limiting side effects. Our data suggests that it might be possible to use low levels of these pan-Nav blockers to reduce seizures without greatly impairing action potential firing in pyramidal neurons. However, it remains to be seen if other pan-Nav blockers will behave in a similar manner, with somewhat mild effects on cell intrinsic excitability whilst reducing seizure activity. Nevertheless, this report demonstrates an important concentration response of seizure-like events to sodium channel inhibition and sets the groundwork for greater understanding of fractional block of compounds required for inhibition of pathological activity, whilst trying to limit their impact on physiological properties of the network.

## Data availability statement

The raw data supporting the conclusions of this article will be made available by the authors, without undue reservation.

## Ethics statement

This animal study was reviewed and approved by Xenon Animal Care Committee, Xenon Pharmaceuticals.

## References

- Armstrong, C. M., and Hille, B. (1998). Voltage-gated ion channels and electrical excitability. *Neuron* 20, 371–380. doi: 10.1016/S0896-6273(00)80981-2
- Bender, A. C., Morse, R. P., Scott, R. C., Holmes, G. L., and Lenck-Santini, P. P. (2012). SCN1A mutations in Dravet syndrome: impact of interneuron dysfunction on neural networks and cognitive outcome. *Epilepsy. Behav.* 23, 177–186. doi: 10.1016/j.yebeh.2011.11.022
- Ben-Shalom, R., Keeshen, C. M., Berrios, K. N., An, J. Y., Sanders, S. J., and Bender, K. J. (2017). Opposing effects on NaV1.2 function underlie differences

## Author contributions

RP and SG conceived this work. AM wrote the analysis code. ST, MW, SL, MS, JM, PV, and RP collected the data. ST, MW, SL, SG, AM, and RP analyzed the data. ST, MW, and RP wrote the manuscript. All authors approved the final draft.

## Funding

This study received funding from Xenon Pharmaceuticals Inc. The funder was not involved in the study design, collection, analysis, interpretation of data, the writing of this article or the decision to submit it for publication.

## Acknowledgments

We thank the entire Xenon family for their support of this work.

## Conflict of interest

ST, MW, SL, AM, JM, MS, and SG are employees of Xenon Pharmaceuticals Inc. and may hold stock or stock options in the company. RP and PV were employees of Xenon Pharmaceuticals Inc.

## Publisher's note

All claims expressed in this article are solely those of the authors and do not necessarily represent those of their affiliated organizations, or those of the publisher, the editors and the reviewers. Any product that may be evaluated in this article, or claim that may be made by its manufacturer, is not guaranteed or endorsed by the publisher.

between SCN2A variants observed in individuals with autism spectrum disorder or infantile seizures. *Biol. Psychiatry* 82, 224–232. doi: 10.1016/j.biopsych.2017.01.009

Brunklaus, A., Ellis, R., Reavey, E., Forbes, G. H., and Zuberi, S. M. (2012). Prognostic, clinical and demographic features in SCN1A mutation-positive Dravet syndrome. *Brain* 135, 2329–2336. doi: 10.1093/brain/aws151

Caldwell, J. H., Schaller, K. L., Lasher, R. S., Peles, E., and Levinson, S. R. (2000). Sodium channel Na(v)1.6 is localized at nodes of ranvier, dendrites, and synapses. *Proc. Natl. Acad. Sci. U.S.A.* 97, 5616–5620. doi: 10.1073/pnas.090034797

- Cammarota, M., Losi, G., Chiavegato, A., Zonta, M., and Carmignoto, G. (2013). Fast spiking interneuron control of seizure propagation in a cortical slice model of focal epilepsy. *J. Physiol.* 591, 807–822. doi: 10.1113/jphysiol.2012.238154
- Catterall, W. A. (1995). Structure and function of voltage-gated ion channels. *Annu. Rev. Biochem.* 64, 493–531. doi: 10.1146/annurev.bi.64.070195.002425
- Catterall, W. A. (2018). Dravet syndrome: a sodium channel interneuronopathy. *Curr. Opin. Physiol.* 2, 42–50. doi: 10.1016/j.cophys.2017.12.007
- Catterall, W. A., Kalume, F., and Oakley, J. C. (2010). Nav1.1 channels and epilepsy. *J. Physiol.* 588, 1849–1859. doi: 10.1113/jphysiol.2010.187484
- Chang, M., Dian, J. A., Dufour, S., Wang, L., Moradi Chameh, H., Ramani, M., et al. (2018). Brief activation of GABAergic interneurons initiates the transition to ictal events through post-inhibitory rebound excitation. *Neurobiol. Dis.* 109, 102–116. doi: 10.1016/j.nbd.2017.10.007
- Cheah, C. S., Yu, F. H., Westenbroek, R. E., Kalume, F. K., Oakley, J. C., Potter, G. B., et al. (2012). Specific deletion of Nav1.1 sodium channels in inhibitory interneurons causes seizures and premature death in a mouse model of Dravet syndrome. *Proc. Natl. Acad. Sci. U.S.A.* 109, 14646–14651. doi: 10.1073/pnas.1211591109
- de Lera Ruiz, M., and Kraus, R. L. (2015). Voltage-gated sodium channels: structure, function, pharmacology, and clinical indications. *J. Med. Chem.* 58, 7093–7118. doi: 10.1021/jm501981g
- Dutton, S. B., Makinson, C. D., Papale, L. A., Shankar, A., Balakrishnan, B., Nakazawa, K., et al. (2013). Preferential inactivation of Scn1a in parvalbumin interneurons increases seizure susceptibility. *Neurobiol. Dis.* 49, 211–220. doi: 10.1016/j.nbd.2012.08.012
- Gardella, E., and Moller, R. S. (2019). Phenotypic and genetic spectrum of SCN8A-related disorders, treatment options, and outcomes. *Epilepsia* 60, S77–S85. doi: 10.1111/epi.16319
- Goldin, A. L., Barchi, R. L., Caldwell, J. H., Hofmann, F., Howe, J. R., Hunter, J. C., et al. (2000). Nomenclature of voltage-gated sodium channels. *Neuron* 28, 365–368. doi: 10.1016/S0896-6273(00)00116-1
- Graham, R. T., Parrish, R. R., Alberio, L., Johnson, E. L., Owens, L. J., and Trevelyan, A. J. (2021). Synergistic positive feedback underlying seizure initiation. *bioRxiv* [Preprint]. doi: 10.1101/2021.02.28.433224
- Guerrini, R., Dravet, C., Genton, P., Belmonte, A., Kaminska, A., and Dulac, O. (1998). Lamotrigine and seizure aggravation in severe myoclonic epilepsy. *Epilepsia* 39, 508–512. doi: 10.1111/j.1528-1157.1998.tb01413.x
- Horn, C. S., Ater, S. B., and Hurst, D. L. (1986). Carbamazepine-exacerbated epilepsy in children and adolescents. *Pediatr. Neurol.* 2, 340–345. doi: 10.1016/0887-8994(86)90074-3
- Hu, H., and Jonas, P. (2014). A supercritical density of Na(+) channels ensures fast signaling in GABAergic interneuron axons. *Nat. Neurosci.* 17, 686–693. doi: 10.1038/nn.3678
- Hu, W., Tian, C., Li, T., Yang, M., Hou, H., and Shu, Y. (2009). Distinct contributions of Na(v)1.6 and Na(v)1.2 in action potential initiation and backpropagation. *Nat. Neurosci.* 12, 996–1002. doi: 10.1038/nn.2359
- Huang, C. J., Schild, L., and Moczydlowski, E. G. (2012). Use-dependent block of the voltage-gated Na(+) channel by tetrodotoxin and saxitoxin: effect of pore mutations that change ionic selectivity. *J. Gen. Physiol.* 140, 435–454. doi: 10.1085/jgp.201210853
- Johannesen, K. M., Gardella, E., Encinas, A. C., Lehesjoki, A. E., Linnankivi, T., Petersen, M. B., et al. (2019). The spectrum of intermediate SCN8A-related epilepsy. *Epilepsia* 60, 830–844. doi: 10.1111/epi.14705
- Johnson, J. P., Focken, T., Khakh, K., Tari, P. K., Dube, C., Goodchild, S. J., et al. (2022). NBI-921352, a first-in-class, Nav1.6 selective, sodium channel inhibitor that prevents seizures in Scn8a gain-of-function mice, and wild-type mice and rats. *eLife* 11:e72468.
- Kaneko, K., Currin, C. B., Goff, K. M., Wengert, E. R., Somarowthu, A., Vogels, T. P., et al. (2022). Developmentally regulated impairment of parvalbumin interneuron synaptic transmission in an experimental model of Dravet syndrome. *Cell Rep.* 38:110580. doi: 10.1016/j.celrep.2022.110580
- Katz, E., Stoler, O., Scheller, A., Khrapunsky, Y., Goebels, S., Kirchhoff, F., et al. (2018). Role of sodium channel subtype in action potential generation by neocortical pyramidal neurons. *Proc. Natl. Acad. Sci. U.S.A.* 115, E7184–E7192. doi: 10.1073/pnas.1720493115
- Kearney, J. A., Plummer, N. W., Smith, M. R., Kapur, J., Cummins, T. R., Waxman, S. G., et al. (2001). A gain-of-function mutation in the sodium channel gene Scn2a results in seizures and behavioral abnormalities. *Neuroscience* 102, 307–317. doi: 10.1016/S0306-4522(00)00479-6
- Khateb, M., Bosak, N., and Herskovitz, M. (2021). The effect of anti-seizure medications on the propagation of epileptic activity: a review. *Front. Neurol.* 12:674182. doi: 10.3389/fneur.2021.674182
- Kuo, C. C., and Bean, B. P. (1994). Slow binding of phenytoin to inactivated sodium channels in rat hippocampal neurons. *Mol. Pharmacol.* 46, 716–725.
- Kuo, C. C., Chen, R. S., Lu, L., and Chen, R. C. (1997). Carbamazepine inhibition of neuronal Na+ currents: quantitative distinction from phenytoin and possible therapeutic implications. *Mol. Pharmacol.* 51, 1077–1083. doi: 10.1124/mol.51.6.1077
- Kwong, K., and Carr, M. J. (2015). Voltage-gated sodium channels. *Curr. Opin. Pharmacol.* 22, 131–139. doi: 10.1016/j.coph.2015.04.007
- Larsen, J., Carvill, G. L., Gardella, E., Kluger, G., Schmiedel, G., Barisic, N., et al. (2015). The phenotypic spectrum of SCN8A encephalopathy. *Neurology* 84, 480–489. doi: 10.1212/WNL.0000000000001211
- Liao, Y., Anttonen, A. K., Liukkonen, E., Gaily, E., Maljevic, S., Schubert, S., et al. (2010). SCN2A mutation associated with neonatal epilepsy, late-onset episodic ataxia, myoclonus, and pain. *Neurology* 75, 1454–1458. doi: 10.1212/WNL.0b013e3181f8812e
- Librizzi, L., Losi, G., Marcon, I., Sessolo, M., Scalmani, P., Carmignoto, G., et al. (2017). Interneuronal Network Activity at the Onset of Seizure-Like Events in Entorhinal Cortex Slices. *J. Neurosci.* 37, 10398–10407. doi: 10.1523/JNEUROSCI.3906-16.2017
- Madeja, M. (2000). Do neurons have a reserve of sodium channels for the generation of action potentials? A study on acutely isolated CA1 neurons from the guinea-pig hippocampus. *Eur. J. Neurosci.* 12, 1–7. doi: 10.1046/j.1460-9568.2000.00871.x
- Magloire, V., Mercier, M. S., Kullmann, D. M., and Pavlov, I. (2019). GABAergic Interneurons in Seizures: Investigating Causality With Optogenetics. *Neuroscientist* 25, 344–358. doi: 10.1177/1073858418805002
- Mahadevan, A., Codadu, N. K., and Parrish, R. R. (2022). Xenon LFP analysis platform is a novel graphical user interface for analysis of local field potential from large-scale MEA recordings. *bioRxiv* [Preprint]. doi: 10.1101/2022.03.25.485521
- Misra, S. N., Kahlig, K. M., and George, A. L. JR. (2008). Impaired Nav1.2 function and reduced cell surface expression in benign familial neonatal-infantile seizures. *Epilepsia* 49, 1535–1545. doi: 10.1111/j.1528-1167.2008.01619.x
- O'Brien, J. E., and Meisler, M. H. (2013). Sodium channel SCN8A (Nav1.6): properties and de novo mutations in epileptic encephalopathy and intellectual disability. *Front. Genet.* 4:213. doi: 10.3389/fgene.2013.00213
- Ogiwara, I., Ito, K., Sawashi, Y., Osaka, H., Mazaki, E., Inoue, I., et al. (2009). De novo mutations of voltage-gated sodium channel alphaII gene SCN2A in intractable epilepsies. *Neurology* 73, 1046–1053. doi: 10.1212/WNL.0b013e3181b9cbe6
- Ogiwara, I., Miyamoto, H., Morita, N., Atapour, N., Mazaki, E., Inoue, I., et al. (2007). Nav1.1 localizes to axons of parvalbumin-positive inhibitory interneurons: a circuit basis for epileptic seizures in mice carrying an Scn1a gene mutation. *J. Neurosci.* 27, 5903–5914. doi: 10.1523/JNEUROSCI.5270-06.2007
- Park, Y. Y., Johnston, D., and Gray, R. (2013). Slowly inactivating component of Na+ current in peri-somatic region of hippocampal CA1 pyramidal neurons. *J. Neurophysiol.* 109, 1378–1390. doi: 10.1152/jn.00435.2012
- Parrish, R. R., Codadu, N. K., Mackenzie-Gray Scott, C., and Trevelyan, A. J. (2019). Feedforward inhibition ahead of ictal wavefronts is provided by both parvalbumin- and somatostatin-expressing interneurons. *J. Physiol.* 597, 2297–2314. doi: 10.1113/jp277749
- Parrish, R. R., Grady, J., Codadu, N. K., Trevelyan, A. J., and Racca, C. (2018). Simultaneous profiling of activity patterns in multiple neuronal subclasses. *J. Neurosci. Methods* 303, 16–29. doi: 10.1016/j.jneumeth.2018.03.012
- Patel, R. R., Ping, X., Patel, S. R., Mcdermott, J. S., Krajewski, J. L., Chi, X. X., et al. (2020). Preferential pharmacological inhibition of Nav1.6, but not Nav1.1, abolishes epileptiform activity induced by 4-AP in mouse cortical slices. *bioRxiv* [Preprint]. doi: 10.1101/2020.05.29.124693
- Pothmann, L., Muller, C., Averkin, R. G., Bellistri, E., Miklitz, C., Uebachs, M., et al. (2014). Function of inhibitory micronetworks is spared by Na+ channel-acting anticonvulsant drugs. *J. Neurosci.* 34, 9720–9735. doi: 10.1523/JNEUROSCI.2395-13.2014
- Raman, I. M., and Bean, B. P. (1999). Ionic currents underlying spontaneous action potentials in isolated cerebellar Purkinje neurons. *J. Neurosci.* 19, 1663–1674. doi: 10.1523/JNEUROSCI.19-05-01663.1999
- Rosker, C., Lohberger, B., Hofer, D., Steinecker, B., Quasthoff, S., and Schreibmayer, W. (2007). The TTX metabolite 4,9-anhydro-TTX is a highly specific blocker of the Na(v)1.6 voltage-dependent sodium channel. *Am. J. Physiol. Cell Physiol.* 293, C783–C789. doi: 10.1152/ajpcell.00070.2007

- Sessolo, M., Marcon, I., Bovetti, S., Losi, G., Cammarota, M., Ratto, G. M., et al. (2015). Parvalbumin-positive inhibitory interneurons oppose propagation but favor generation of focal epileptiform activity. *J. Neurosci.* 35, 9544–9557. doi: 10.1523/JNEUROSCI.5117-14.2015
- Seutin, V., and Engel, D. (2010). Differences in Na<sup>+</sup> conductance density and Na<sup>+</sup> channel functional properties between dopamine and GABA neurons of the rat substantia nigra. *J. Neurophysiol.* 103, 3099–3114. doi: 10.1152/jn.00513.2009
- Shiri, Z., Manseau, F., Levesque, M., Williams, S., and Avoli, M. (2015). Interneuron activity leads to initiation of low-voltage fast-onset seizures. *Ann. Neurol.* 77, 541–546. doi: 10.1002/ana.24342
- Spratt, P. W. E., Alexander, R. P. D., Ben-Shalom, R., Sahagun, A., Kyoung, H., Keeshen, C. M., et al. (2021). Paradoxical hyperexcitability from NaV1.2 sodium channel loss in neocortical pyramidal cells. *Cell Rep.* 36:109483. doi: 10.1016/j.celrep.2021.109483
- Swensen, A. M., and Bean, B. P. (2005). Robustness of burst firing in dissociated purkinje neurons with acute or long-term reductions in sodium conductance. *J. Neurosci.* 25, 3509–3520. doi: 10.1523/JNEUROSCI.3929-04.2005
- Tian, C., Wang, K., Ke, W., Guo, H., and Shu, Y. (2014). Molecular identity of axonal sodium channels in human cortical pyramidal cells. *Front. Cell Neurosci.* 8:297. doi: 10.3389/fncel.2014.00297
- Trevelyan, A. J., Sussillo, D., Watson, B. O., and Yuste, R. (2006). Modular propagation of epileptiform activity: evidence for an inhibitory veto in neocortex. *J. Neurosci.* 26, 12447–12455. doi: 10.1523/JNEUROSCI.2787-06.2006
- Trimmer, J. S., and Rhodes, K. J. (2004). Localization of voltage-gated ion channels in mammalian brain. *Annu. Rev. Physiol.* 66, 477–519. doi: 10.1146/annurev.physiol.66.032102.113328
- Tsukamoto, T., Chiba, Y., Wakamori, M., Yamada, T., Tsunogae, S., Cho, Y., et al. (2017). Differential binding of tetrodotoxin and its derivatives to voltage-sensitive sodium channel subtypes (Nav 1.1 to Nav 1.7). *Br. J. Pharmacol.* 174, 3881–3892. doi: 10.1111/bph.13985
- Wang, J., Ou, S. W., and Wang, Y. J. (2017). Distribution and function of voltage-gated sodium channels in the nervous system. *Channels* 11, 534–554. doi: 10.1080/19336950.2017.1380758
- Yekhhlef, L., Breschi, G. L., Lagostena, L., Russo, G., and Taverna, S. (2015). Selective activation of parvalbumin- or somatostatin-expressing interneurons triggers epileptic seizurelike activity in mouse medial entorhinal cortex. *J. Neurophysiol.* 113, 1616–1630. doi: 10.1152/jn.00841.2014
- Yu, F. H., Mantegazza, M., Westenbroek, R. E., Robbins, C. A., Kalume, F., Burton, K. A., et al. (2006). Reduced sodium current in GABAergic interneurons in a mouse model of severe myoclonic epilepsy in infancy. *Nat. Neurosci.* 9, 1142–1149. doi: 10.1038/nn1754
- Zhang, M. M., Wilson, M. J., Azam, L., Gajewiak, J., Rivier, J. E., Bulaj, G., et al. (2013). Co-expression of Na(V)β subunits alters the kinetics of inhibition of voltage-gated sodium channels by pore-blocking mu-conotoxins. *Br. J. Pharmacol.* 168, 1597–1610. doi: 10.1111/bph.12051
- Zuliani, V., Patel, M. K., Fantini, M., and Rivara, M. (2009). Recent advances in the medicinal chemistry of sodium channel blockers and their therapeutic potential. *Curr. Top. Med. Chem.* 9, 396–415. doi: 10.2174/156802609788317856